

Supplementary Materials

UTMD-Promoted Co-Delivery of Gemcitabine and miR-21 Inhibitor by Dendrimer-Entrapped Gold Nanoparticles for Pancreatic Cancer Therapy

Lizhou Lin^{1#}, Yu Fan^{2#}, Feng Gao¹, Lifang Jin¹, Dan Li², Wenjie Sun², Fan Li¹, Peng Qin⁴, Qiusheng Shi^{1*}, Xiangyang Shi^{2,3*}, Lianfang Du^{1*}

¹ Department of Ultrasound, Shanghai General Hospital, Shanghai Jiaotong University School of Medicine, Shanghai 200080, P. R. China

² College of Chemistry, Chemical Engineering and Biotechnology, Donghua University, Shanghai 201620, P. R. China

³ CQM-Centro de Química da Madeira, Universidade da Madeira, Campus da Penteada, 9000-390 Funchal, Portugal

⁴ Department of Instrument Science and Engineering, Shanghai Jiao Tong University, Shanghai, 201108, China

* Corresponding Authors: E-mail: dulf_sh@163.com (L. Du), sqs19631989@163.com (Q. Shi) and xshi@dhu.edu.cn (X. Shi)

Authors contributed equally to this work.

Experimental Details

Materials and reagents

Ethylenediamine core amine-terminated G5 PAMAM dendrimers were purchased from Dendritech (Midland, MI). PEG monomethyl ether with the other end of carboxyl group (*m*PEG-COOH, $M_w = 2000$) were purchased from Shanghai Yanyi Biotechnology Corporation (Shanghai, China). Gemcitabine (Gem), acetic anhydride, triethylamine, 1-(3-dimethylaminopropyl)-3-ethylcarbodiimide hydrochloride (EDC HCl), N-hydroxysuccinimide (NHS), fluorescein isothiocyanate (FITC), $\text{HAuCl}_4 \cdot 4\text{H}_2\text{O}$ and other chemicals and solvents were provided by Sigma-Aldrich (St. Louis, MO). SW1990 cells (a human pancreatic cancer cell line) were obtained from Institute of Biochemistry and Cell Biology, the Chinese Academy of Sciences (Shanghai, China). Roswell Park Memorial Institute (RPMI) 1640 medium, fetal bovine serum (FBS), penicillin and streptomycin were purchased from Gibco (Carlsbad, CA). Commercial SonoVue was purchased from Bracco (Milan, Italy). 2'-O-Methyl miR-21 inhibitor (sequence: 5'-UCA ACA UCA GUC UGA UAA GCU A -3') and Cy-3-labeled miR-21 inhibitors were supplied by Shanghai Gene Pharma (Shanghai, China). Water used in all experiments was purified using a Milli-Q Plus 185 water purification system (Millipore, Bedford, MA) with a resistivity higher than 18.2 $\text{M}\Omega\cdot\text{cm}$. Regenerated cellulose dialysis membranes with a molecular weight cut-off (MWCO) of 3000 or 10,000 were acquired from Fisher Scientific (Philadelphia, PA).

Synthesis of G5.NH₂-*m*PEG

*m*PEG-COOH (24.28 mg, 11.5 mmol), EDC HCl (44.22 mg, 23.07 mmol), and NHS (26.55mg, 23.07 mmol) were co-dissolved in dimethyl sulfoxide (DMSO, 2 mL), and the reaction mixture was stirred for 3 h at room temperature. The activated *m*PEG-COOH was then dropwise added to a solution of G5.NH₂ (20.00 mg, 0.77 mmol) dissolved in DMSO (3 mL) under vigorous magnetic stirring for 24 h to obtain the raw product of G5.NH₂-*m*PEG. Then, the reaction mixture was extensively dialyzed against water (9 times, 2 L) through a 3000 MWCO dialysis membrane for 3 days to remove the excess of reactants, followed by lyophilization to get the product of G5.NH₂-*m*PEG.

Synthesis of $\{(Au^0)_{25}\text{-G5.NH}_2\text{-}m\text{PEG}\}$ DENPs

G5.NH₂-*m*PEG dendrimers were used as templates to synthesize dendrimer-entrapped Au nanoparticles (Au DENPs) *via* sodium borohydride reduction chemistry with the molar ratio of gold salt to G5.NH₂-*m*PEG at 25:1. Briefly, the HAuCl₄ solution (127 μL in water, 30 mg/mL) was dropwise added to an aqueous solution of the G5.NH₂-*m*PEG dendrimer (20 mg, 20 mL) under vigorous magnetic stirring. After 30 min, an ice cold NaBH₄ solution (176 μL in water, 10 mg/mL) was rapidly added to the gold salt/dendrimer mixture under stirring. The reaction mixture turned deep-red within a few seconds. The stirring was continued for 3 h to obtain the raw product of $\{(Au^0)_{25}\text{-G5.NH}_2\text{-}m\text{PEG}\}$ DENPs. Then, the reaction mixture was extensively dialyzed against water (9 times, 2 L) through a 10,000 MWCO dialysis membrane for 3 days to remove the excess of reactants, followed by lyophilization to get the product of $\{(Au^0)_{25}\text{-G5.NH}_2\text{-}m\text{PEG}\}$ DENPs.

Characterization of $\{(Au^0)_{25}\text{-G5.NH}_2\text{-}m\text{PEG}\}$ DENPs

UV-vis spectra were recorded using a Lambda 25 UV-vis spectrophotometer (PerkinElmer, Boston, MA). All samples were dissolved in water before measurements. TEM was performed using a JEOL 2010F analytical electron microscope (JEOL, Tokyo, Japan) with an accelerating voltage of 200 kV. TEM samples were prepared by depositing an aqueous suspension of Au DENPs (5 μL, 3 mg/mL) onto a carbon coated copper grid and air-dried before observation. Image J software was used to analyze the size and size distribution of each sample. At least 200 Au DENPs randomly selected from different TEM images were measured for each sample. To determine the number of the terminal primary amine groups present on the surface of Au DENPs, Megazyme's PANOPA Assay Kit was used and the assays were performed according to the manufacturer's instructions.

Preparation of Gem-loaded Au DENPs

To load Gem onto the Au DENPs, Gem and Au DENPs were mixed together in PBS and sonicated for 15 min, then the aqueous solution was stirred for 24 h. After that, the mixture solution was centrifuged (7500 rpm, 5 min) for 3 times to remove the free Gem through a Centricon device (Millipore, 4 mL/10 KD). The concentrated solution was collected and then lyophilized to obtain the Gem-Au DENPs complexes. The free Gem was collected and diluted with PBS and measured *via*

UV-vis spectroscopy to quantify the amount of non-encapsulated Gem.

***In vitro* release assay**

Gem and Gem-Au DENPs complexes were separately dispersed in PBS and then placed in a dialysis bag with an MWCO of 10,000 in a vapor-bathing constant temperature vibrator at 37 °C. The dialysis bag was hermetically tied, immersed in 25 mL of PBS, and stirred continuously. At each scheduled time interval, 1 mL of sample was collected from the outer phase buffer medium for UV-vis spectroscopic analysis. In addition, 1 mL of the corresponding buffer medium was replenished.

Cell culture

SW1990 cells were regularly maintained in RPMI 1640 medium supplemented with FBS (10%), penicillin (100 U/mL) and streptomycin (100 mg/ml) in a 37 °C humidified incubator containing 5% CO₂. When the cell concentration reached more than 1×10^6 cells/mL, cells were re-suspended in PBS for ultrasound exposure experiments.

Preparation of Sonovue microbubbles

Sonovue, an ultrasound contrast agent (UCA) containing stabilized microbubbles filled with SF₆ gas were used. The microbubbles' diameter ranged from 1.5 to 3.0 μM with the shell composed of lipid monolayer membrane. According to the manufacture's instruction, the Sonovue suspension containing $2-5 \times 10^8$ microbubbles/mL was prepared.

Ultrasound (US) exposure apparatus

The cavitation experiments were performed in a US exposure device. The acoustic apparatus fixed in a tank filled with water at room temperature, where a tube was used to hold the cell suspension and was fixed at a customized bracket. A Topteam161 Physioson-Basic therapeutic US machine (Physioson Elektromedizin AG, Laipersdorf, Germany) with a 20.4-mm diameter ultrasound probe was installed on the horizontal plane of this tank at a distance of about 80 mm from the incident surface of the transducer [1].

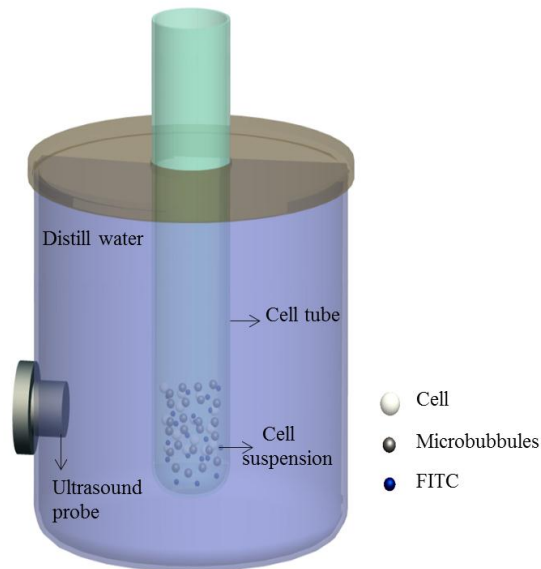


Figure S1. Experimental apparatus for acoustic cavitation experiments. The cell tube was installed in the tank filled with water.

Real-time PCR

Total RNA was extracted from cells using Trizol reagent (Invitrogen) and was performed with the mirVana qRT-PCR miRNA detection kit (TAKARA) in a 10 μ L reaction mixture. Amplification reaction was carried out using 7500 fast real-time PCR (Roche) and the protocol was performed for 40 cycles at 37 °C for 15 min, 85 °C for 5 s, and 4 °C for 60 s. Relative quantification was conducted using amplification efficiencies derived from 2nd-Strand cDNA. Data are gained as fold changes ($2^{-\Delta\Delta C_t}$) and were analyzed using Opticon Monitor Analysis Software V 2.02 (Thermal, Waltham, MA).

Dynamic fluorescence biodistribution of Gem-Au DENPs/miR-21i

To investigate the biodistribution of polypeptides delivery and enhanced retention combined with UTMD, a small animal *in vivo* fluorescence imaging system (LuminaXRMS; PerkinElmer, Walther, MA, USA) was applied. Gem-Au DENPs/Cy3-miR-21i polyplexes at a dose of 10 mg/kg were injected through the tail vein. For the groups of Gem-Au DENPs/Cy3-miR-21i plus UTMD (Gem-Au DENPs/Cy3-miR-21i + U), the US transducer (PHYSIOSON-Basic, PHYSIOSON Elektro-medizin, Germany) was positioned above the tumor, and SonoVue (1.18 mg/mL, in 0.2 mL saline) was slowly injected via tail vein after intratumoral injection of Gem-Au DENPs/miR-21i

polyplexes. The real-time imaging was performed by the small animal *in vivo* fluorescence imaging system at the time intervals of 0.5 h, 4 h, 8 h, and 12 h. The dynamic change of fluorescence biodistribution was recorded.

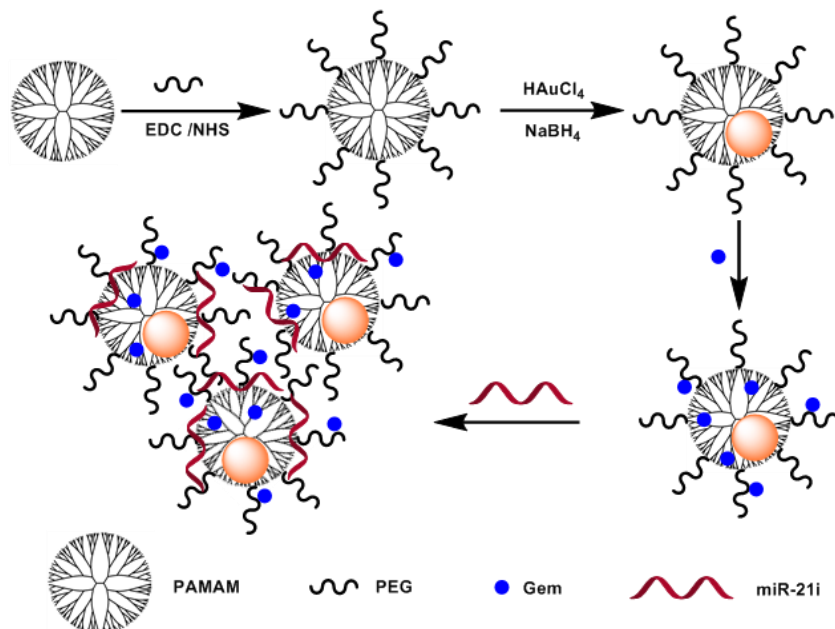
Pharmacokinetics of Gem-Au DENPs/miR-21i

For pharmacokinetics investigations, mice with a subcutaneous tumor in the three groups of free Gem, Gem-Au DENPs/miR-21i and Gem-Au DENPs/miR-21i + U were given the same Gem dose of 10mg Gem/Kg through the tail vein. At 0.5 h, 1 h, 4 h, 8 h, 12 h and 24 h after drug injection, blood samples from the free Gem, Gem-Au DENPs/miR-21i and tumor samples from all groups were collected. The samples were further investigated into plasma and tissue respectively, and the Gem concentrations were subsequently detected by liquid chromatography/mass spectrometry (Thermo Scientific TSQ Quantum Ultra; Massachusetts, USA). The pharmacokinetics analysis was conducted by Das 2.0 software with non-compartmental modeling and the parameters including AUC, $t_{1/2}$ (half time), MRT (mean residence time) and C_{max} (maximal concentration). The Gem level in the tumor was also calculated and represented the total drug accumulated in the tumor within 24 h.

Results and discussion

Characterization of G5.NH₂-*m*PEG

The chemical structure of G5.NH₂-*m*PEG was characterized by ¹H NMR (Fig. S2). The characteristic PEG methylene proton peak was located at 3.6 ppm. Based on the integration of the relevant peaks in the ¹H NMR spectrum [2], the number of PEG moieties attached onto each G5 dendrimer was estimated to be 14.



Scheme S1. Schematic illustration of the synthesis of the Au DENPs for co-delivery of Gem and miR-21i.

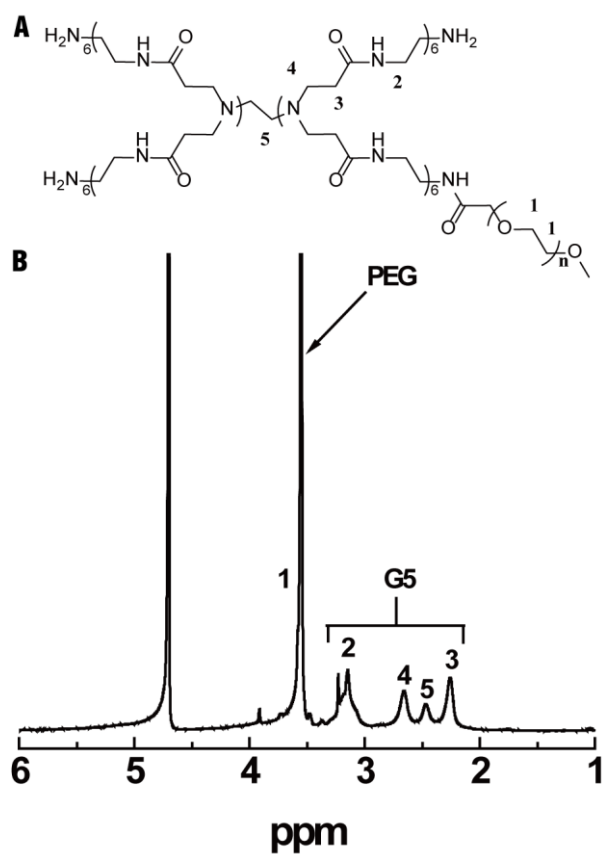


Figure S2. ^1H NMR of G5.NH₂-mPEG.

Characterization of Gem-Au DENPs polyplexes

The formed Gem-Au DENPs polyplexes were characterized by UV-vis spectroscopy (Fig. S3). The appearance of an absorption peak at 260 nm can be assigned to the characteristic absorption of Gem, indicating that Gem has been successfully loaded within the Au DENPs.

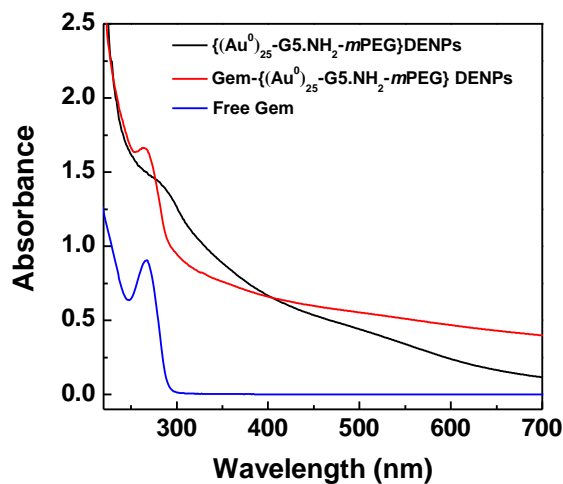


Figure S3. UV-vis absorbance spectra of $\{(Au^0)_{25}-G5.NH_2-mPEG\}$ DENPs (black), Free Gem (blue) and Gem- $\{(Au^0)_{25}-G5.NH_2-mPEG\}$ DENPs (red).

The Gem payload within the Au DENPs was analyzed with UV-vis spectroscopy using a standard Gem absorbance/concentration calibration curve (Fig. S4A). To achieve Gem-loaded Au DENPs with satisfying entrapment efficiency (EE) and drug loading percentage (DL), molar ratio of Gem to Au DENPs was optimized (Table S1). Finally, we chose the highest EE with molar ratio of Gem to Au DENPs at 100:1, and there are 38.79 Gem molecules complexed within each Au DENP. To explore its anticancer therapeutic efficacy, the Gem encapsulated within the Au DENPs should be able to be released. According to the drug release curve (Fig. S4B), $46.68 \pm 5.10\%$ Gem can be released from the complexes after 3 h. In contrast, free Gem can be quickly released and $90.03\% \pm 3.79\%$ Gem is released after 3 h. This indicated that the Gem encapsulated within the Au DENPs can be released in a sustained manner, in agreement with the literature [3, 4].

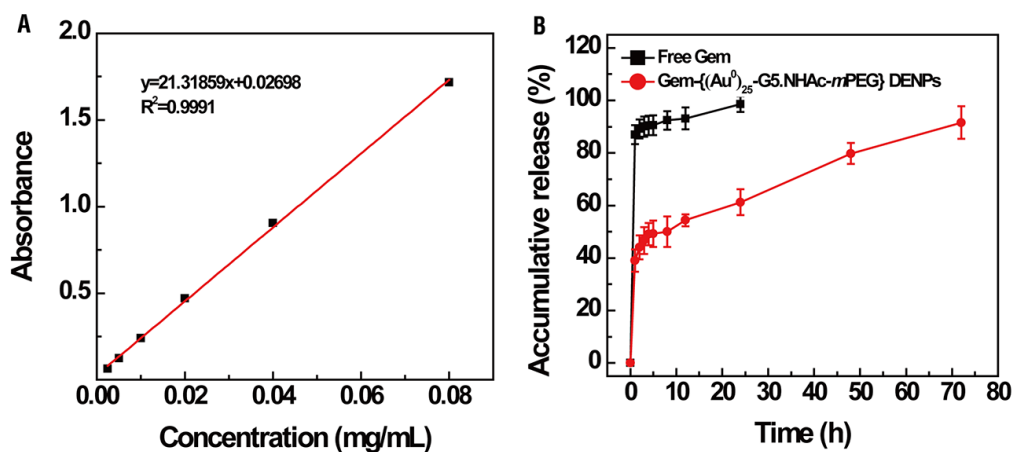


Figure S4. (A) The calibration curve of Gem absorbance/concentration. (B) The release of Gem from Gem/((Au⁰)₂₅-G5.NH₂-mPEG) DENPs complexes as a function of time. Free Gem was used as control. PBS (pH 7.4) was used as the release medium.

Table S1. Results of encapsulation efficiency and drug loading.

Gem/Au DENPs	EE (%)	DL (eq)
300/1	15.11 ± 3.09	16.90 ± 3.45
150/1	33.34 ± 5.46	18.32 ± 3.00
100/1	38.79 ± 3.03	14.82 ± 1.15

Cytotoxicity assay of Au DENPs and Au DENPs/miR-21i

SW1900 cells treated with Au DENPs at different concentrations display higher cell viability than 80% at 72 h, indicating their good cytocompatibility in the studied concentration range. To check the gene therapy efficacy of the Au DENPs/miR-21i polyplexes, we tested the viability of cells treated with Au DENPs/miR-21i polyplexes ([miR-21i] = 20 μM). It can be seen that the cells show a lower viability at a longer time period and the cell viability still remains a high level (> 70%) even after 72 h treatment in the studied concentration range. This suggests that single mode of gene therapy is quite weak.

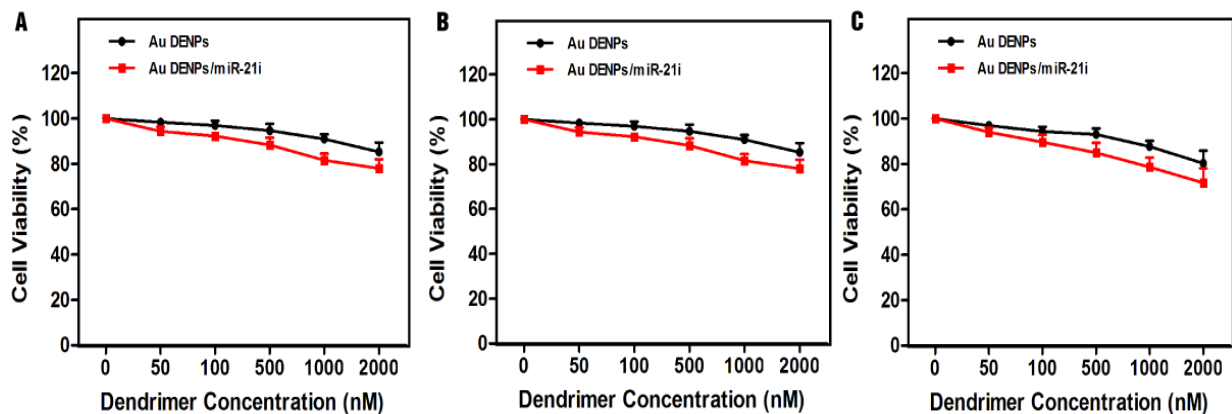


Fig S5. CCK-8 viability assay of cells treated with Au DENPs and Au DENPs/miR-21i polyplexes at different concentrations for (A) 24 h, (B) 48 h, and (C) 72 h.

Cellular uptake assays

The fluorescent intensity was quantitative by flow cytometry analysis. Fig. S6 shows the cellular uptake of Gem-Au DENPs/Cy3-miR-21i complexes as reflected by the fluorescence intensity of cells. The cellular uptake of the polyplexes displays a time-dependent manner with a longer time period having enhanced cellular uptake of the polyplexes. At the time point of 4 h, the cells treated with UTMD have further enhanced uptake of the polyplexes when compared with those without UTMD treatment.

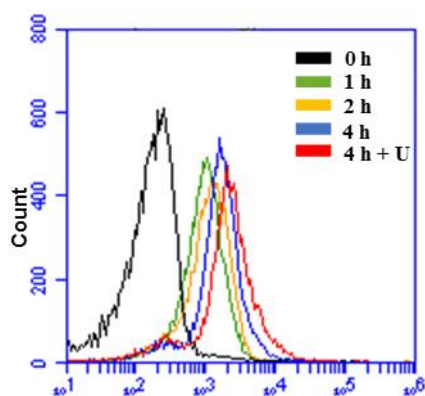


Figure S6. Flow cytometric assay of the cells treated with the Gem-Au DENPs/Cy3-miR-21i polyplexes at different time points. For the 4 h treatment, the cells were also UTMD treated.

PCR analysis

Real-time PCR was carried out to further confirm the cell apoptosis response. These results show that PTEN, P53 and Bax were dramatically increased in Gem-Au DENPs/miR-21i + U group. The anti-apoptotic protein Bcl-2 was substantially decreased. This indicates the activation of the mitochondrial apoptosis pathway, in accordance with western blot analysis.

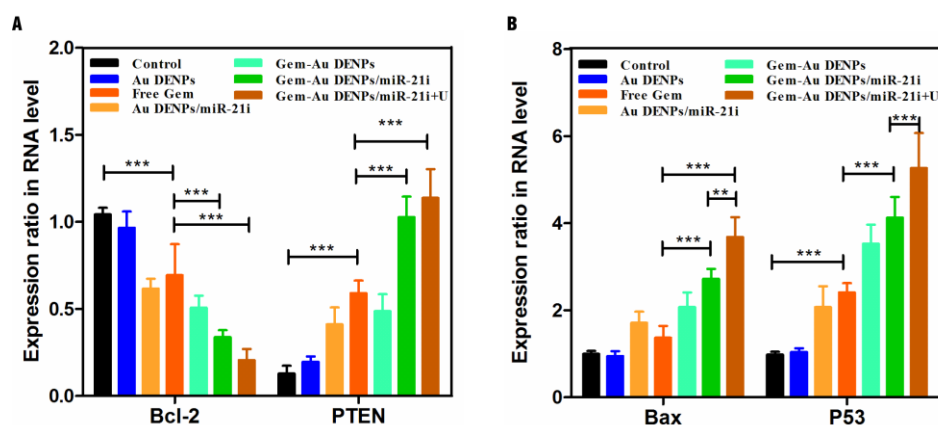


Figure S7. Real-time PCR analysis of gene expression levels with (A) Bcl-2 and PTEN, and (B) Bax and P53 under different treatment conditions.

Dynamic fluorescence biodistribution of Gem-Au DENPs/miR-21i in mouse pancreatic tumor xenografts

To study the biodistribution of Gem-Au DENPs/miR-21i polyplexes and the enhanced efficiency of UTMD, a small animal *in vivo* fluorescence imaging system was used to detect the accumulation of Cy3 in the subcutaneous tumor model in BALB/c nude mice. During the first 0.5 h post-injection, the fluorescence of Cy3 mainly distributed throughout the body. The signal intensity of the Cy3 fluorescence in tumor reached peak levels at 4 h in groups with NPs, in addition, the signal of the Cy3 fluorescence in Gem-Au DENPs/miR-21i + U group was higher than the Gem-Au DENPs/miR-21i group. In the free Cy3 group, the fluorescence was barely observed in the tumor at 8 h and became very weak to be detected in the whole body at 12 h. However, the fluorescence in the tumor still can be obviously observed in other two groups (Fig. S8). The reason for longer retention time might be due to that the Au DENPs could escape from the reticuloendothelial system

(RES) and stay longer in circulation. Furthermore, the Cy3 fluorescence in tumor with UTMD group was lasting much longer in compared with Gem-Au DENPs/miR-21i group and decreased gradually. Also, the intensity of Cy3 fluorescence in tumor of Gem-Au DENPs/miR-21i group was still higher than that without UTMD group at 8 h. This enhanced efficiency of UTMD was similar to the cellular uptake *in vitro*, and the fluorescent signal increased by the effect of sonoporation and lasting over a few hours. Taken together, these results demonstrated that the accumulation of Gem-Au DENPs/miR-21i in tumors was significantly increased by Au DENPs and further enhanced by UTMD in pancreatic tumor xenografts.

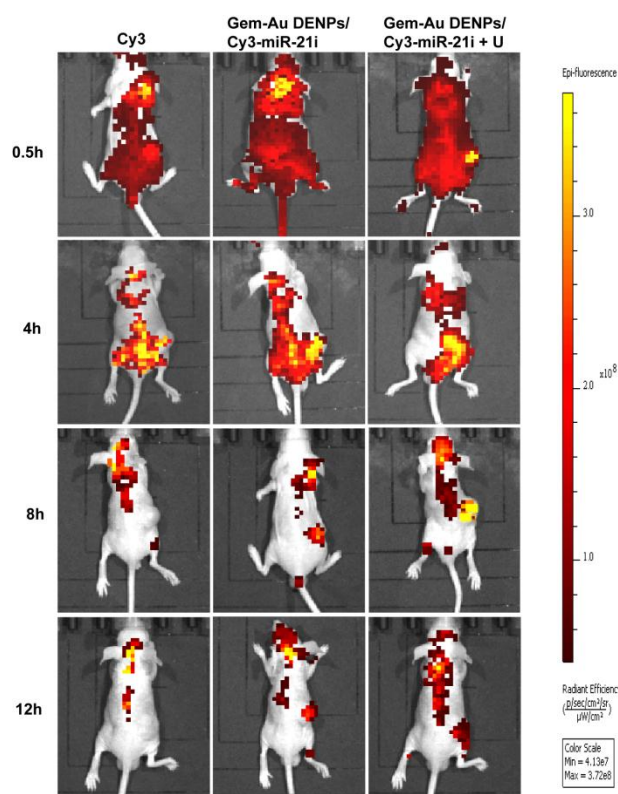


Figure S8. Dynamic fluorescence biodistribution of Gem-Au DENPs/Cy3-miR-21i polyplexes. Different time intervals of 0.5 h, 4 h, 8 h and 12 h were carried out after administration of free Cy3, Gem-Au DENPs/Cy3-miR-21i and Gem-Au DENPs/Cy3-miR-21i + U.

***In vivo* pharmacokinetic evaluation**

We further evaluated the pharmacokinetics in mouse pancreatic tumor xenografts. The result of Gem concentrations in plasma and tumors are shown in Fig.S9 and the pharmacokinetic parameters

are listed in Table S2. Fig. S9A illustrated the differences in blood drug level between free Gem and Gem-Au DENPs/miR-21i, particularly in the period from 0.5 to 8 h ($p < 0.05$). Compared with free Gem, Gem-Au DENPs/miR-21i improved the pharmacokinetic profile of Gem by increasing $t_{1/2}$, AUC, MRT and C_{max} . The results of $t_{1/2}$ and MRT revealed that Au DENPs can prolong the in vivo circulation time of the drug. This performance may be due to the ability of Au DENPs evade the RES to have longer circulation. The C_{max} and AUC values of the Gem-Au DENPs/miR-21i were 1.75-fold and 3.44-fold higher, respectively, compared to the free drug, demonstrating sustained drug release ability and longer duration in circulation (Table S2). Over the first 4 h, significant differences of blood drug levels between the free Gem and Gem-Au DENPs/miR-21i could be observed, at the same time, the fluorescence in the tumors of Gem-Au DENPs/Cy3-miR-21i remained high while it significantly decreased in the free Cy3 group, demonstrated that the Gem-Au DENPs/miR-21i had a more ideal in vivo pharmacokinetic profile. To further investigate the enhanced effect of UTMD for the Gem accumulation in the tumor, we tested the Gem concentration at different time intervals following the administration of Gem-Au DENPs/miR-21i with and without UTMD. Fig. S9B showed that the concentration of Gem rose sharply and reached a higher level earlier than that with polyplexes alone. This result was predictable due to the sonoporation effect by UTMD which facilitates the delivery of polyplexes by the repairable pores and the profiles of pharmacokinetic were in agreement with the results obtained by dynamic fluorescence biodistribution.

Table S2: Pharmacokinetic parameters of free Gem and Gem-Au DENPs/miR-21i in non-compartmental modeling by Das.2.0.

	Free Gem	Gem-Au DENPs/miR-21i	<i>p</i>
$t_{1/2\beta}$ (h)	2.12 ± 0.48	6.15 ± 0.53	<0.0001
C_{max} (µg/mL)	6.65 ± 0.55	11.65 ± 0.71	<0.0001
AUC _{0-∞} (µg/mL•h)	28.67 ± 6.41	98.67 ± 10.23	<0.0001
MRT (h)	2.68 ± 0.38	8.32 ± 0.44	<0.0001

$t_{1/2}$, half-life; C_{max} , maximal concentration; AUC, area under the curve; MRT, mean residence time.

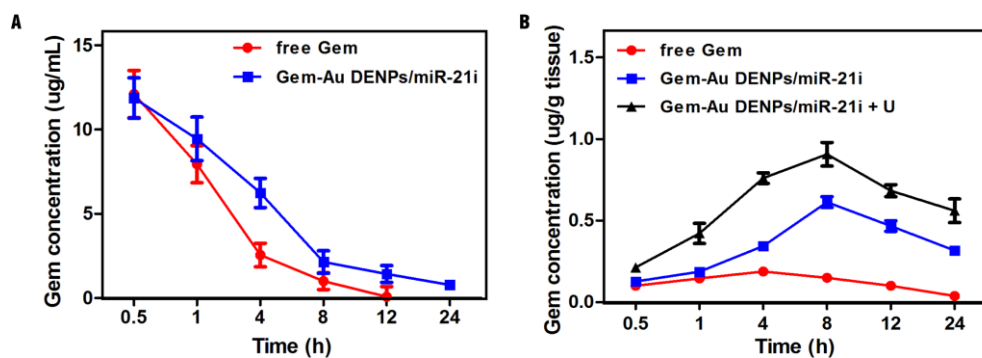


Figure S9. Pharmacokinetics of Gem after intravenous injection of Gem, Gem-Au DENPs/miR-21i and Gem-Au DENPs/miR-21i + U: Concentration of Gem in (A) plasma and (B) tumors. Data are presented as mean \pm SD (n=3).

Therapeutic effect *in vivo*

Finally, we used CEUS imaging to further investigate the therapeutic effect of Gem-Au DENPs/miR-21i by intravenously injected routine. As Fig. S10 shown, the tumor size and blood flow in the UTMD group had slight increased, indicating that the UTMD conditions used in this study are mainly to promote cellular uptake and increase local drug concentration. In Gem-Au DENPs/miR-21i group, the tumor size kept constant after treatment. While in the Gem-Au DENPs/miR-21i + U group it showed a slight decrease in tumor size and a more obvious blood flow when compared to without UTMD group, which it may be related to the effect of UTMD enhance gemcitabine treatment in pancreatic cancer.

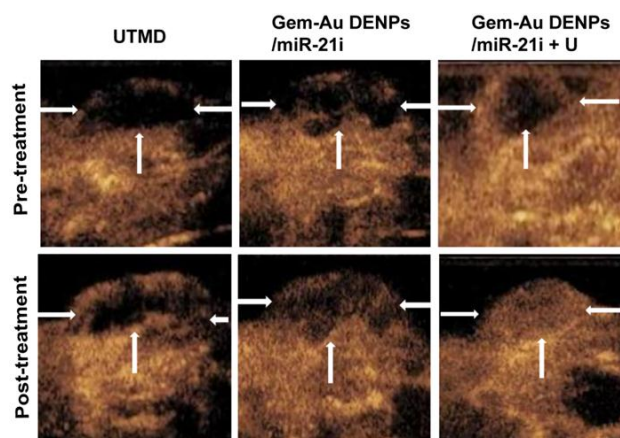


Figure S10. The CEUS imagings of UTMD, Gem-Au DENPs/miR-21i and Gem-Au DENPs/miR-21i + U groups in the pre-treatment and post-treatment.

***In vivo* histological analysis of mouse organs**

To evaluate the *in vivo* toxicity caused by the co-delivery platform under UTMD treatment, the main organs of mice were H&E stained and observed by optical microscopy. No obvious adverse effects to the major organs of mice were found after the mice were treated with Gem-Au DENPs/Cy3-miR-21i + U at 21 days post-injection.

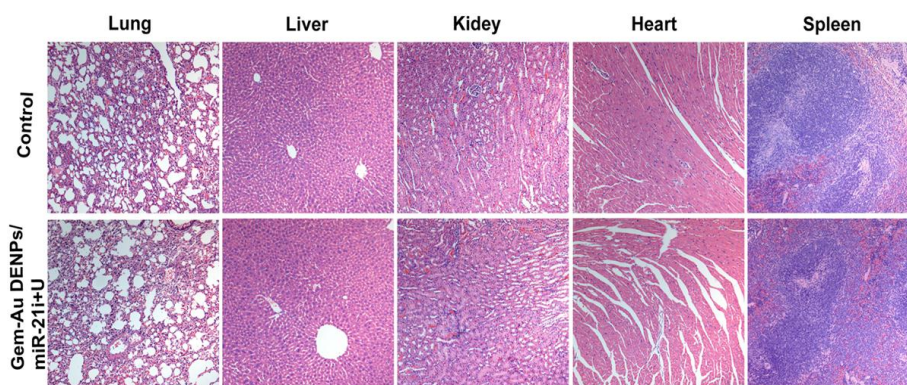


Figure S11. H&E staining of the major organs of mice after the mice were treated with Gem-Au DENPs/Cy3-miR-21i + U for 21 days.

References

1. Lin Y, Lin L, Cheng M, Jin L, Du L, Han T, et al. Effect of acoustic parameters on the cavitation behavior of SonoVue microbubbles induced by pulsed ultrasound. *Ultrason Sonochem.* 2017; 35: 176-184.
2. Peng C, Qin J, Zhou B, Chen Q, Shen M, Zhu M, et al. Targeted tumor CT imaging using folic acid-modified PEGylated dendrimer-entrapped gold nanoparticles. *Polymer Chem.* 2013; 4: 4412-4424.
3. Wang Y, Guo R, Cao X, Shen M, Shi X. Encapsulation of 2-methoxyestradiol within multifunctional poly(amidoamine) dendrimers for targeted cancer therapy. *Biomaterials.* 2011; 32: 3322-3329.
4. Wang Y, Cao X, Guo R, Shen M, Zhang M, Zhu M, et al. Targeted delivery of doxorubicin into cancer cells using a folic acid–dendrimer conjugate. *Polymer Chem.* 2011; 2: 1754-1760.